ELSEVIER

Engineering Analysis with Boundary Elements 23 (1999) 683–691

ENGINEERING ANALYSIS *with* BOUNDARY ELEMENTS

www.elsevier.com/locate/enganabound

Boundary element analysis of fracture mechanics in anisotropic bimaterials

E. Pan[a,*], B. Amadei[b]

[a]*Department of Mechanical Engineering, University of Colorado at Boulder, Boulder, CO 80309-0427, USA*
[b]*Department of Civil Engineering, University of Colorado at Boulder, Boulder, CO 80309-0427, USA*

Received 9 November 1998; accepted 7 April 1999

Abstract

This paper presents a boundary element formulation for the analysis of linear elastic fracture mechanics problems involving anisotropic bimaterials. The most important feature associated with the present formulation is that it is a single domain method, and yet it is accurate, efficient and versatile. In this formulation, the displacement integral equation is collocated on the uncracked boundary only, and the traction integral equation is collocated on one side of the crack surface only. The complete Green's functions for anisotropic bimaterials are also derived and implemented into the boundary integral formulation so that discretization along the interface can be avoided except for the interfacial crack part. A special crack-tip element is introduced to capture exactly the crack-tip behavior.

Numerical examples are presented for the calculations of stress intensity factors for a straight crack with various locations in infinite bimaterials. It is found that very accurate results can be obtained by the proposed method even with relatively coarse discretization. Numerical results also show that material anisotropy can greatly affect the stress intensity factor.

Keywords: Fracture mechanics; Anisotropic bimaterials; Crack-tip behavior

1. Introduction

Fracture mechanics in bimaterials is getting increasing attention because of its direct applications to composite laminates which are widely used in aircraft and space structures. It is well known that laminated structures are prone to defects such as broken fibers, cracks in the matrix material, and interface delaminating. Premature failure due to the existence of delamination is one of the most common failure modes in composite materials and bonded joints.

Theoretically, interfacial crack problems in isotropic bimaterials were studied [1–3] where the authors showed that the stresses possess the singularity of $r^{-1/2\pm i\varepsilon}$. Rice [4] re-examined the elastic fracture mechanics concepts for the isotropic interfacial crack and introduced an intrinsic material length scale so that the definition of the stress intensity factor (SIF) possesses the same physical significance as those for the homogeneous cracks. Clements [5] and Willis [6] studied interfacial crack problems in dissimilar anisotropic materials. They showed that the oscillatory behavior of the stresses and the phenomenon of interpenetrating of the crack faces were also present near the crack-tips for anisotropic interface cracks. Recent studies on interfacial cracks in anisotropic materials have been conducted by many authors [7–16] and different definitions for the stress intensity factor exist. By introducing a characteristic length, however, the definition given by Wu [12,13] and Gao et al. [16] is consistent with Rice's general definition [4] and appears to be more explicit than other definitions.

The Boundary element method (BEM) is particularly suited to cases where better accuracy is required due to problems such as stress concentrations at the crack-tip. Another important feature associated with the BEM is that it only requires discretization of the boundary rather than the domain. Previously, the BEM has been applied to interfacial cracks in isotropic bimaterials [17,18] and in anisotropic bimaterials [19,20]. It is noted that, however, in these previous BEM formulations, the Green's functions in an infinite-plane were used, which therefore require discretization along the interface. Although Yuuki and Cho [17] used Hetenyi's solution for isotropic bimaterials, their BEM formulation still requires the subdivision of the whole bimaterial domain. Furthermore, the off-interface crack or the crack across the interface in bimaterials cannot be studied easily with their BEM formulations.

* Corresponding author.

0955-7997/99/$ - see front matter
PII: S0955-7997(99)00018-1

In this paper, we present a BEM formulation for the analysis of linear elastic fractures in anisotropic bimaterials. First, we derive the complete Green's functions for anisotropic bimaterials and show their implementation into our BEM formulation so that discretization along the interface is avoided except for the interfacial crack part. Since the interfacial crack has an oscillation singular behavior, we introduce a special crack-tip element to exactly capture this behavior. The most important feature of the present analysis is that it is a single-domain method, and yet it is accurate, efficient and versatile. This single-domain formulation resembles the dual boundary element method [21–23] and is a direct extension of the authors' recent BEM work for homogeneous and anisotropic media [24,25] where the displacement and traction integral equations are collocated, respectively, on the uncracked boundary only and on one side of the crack surface only.

Calculation of the SIFs is conducted for several situations, like cracks along or off an interface. Numerical results show that the proposed method is very accurate even with relatively coarse mesh discretization. This is the first time that the single-domain BEM method developed for homogeneous media has been extended to the bimaterial case.

2. Green's functions in anisotropic bimaterials

The complex variable function method has been found to be very suitable for the study of 2D anisotropic elastic media [26]. Notably, Eshelby et al. [27], Stroh [28] and Lekhnitskii [26] have studied the Green's functions in infinite planes using the complex function method. The complete Green's functions in an elastic, anisotropic, and infinite-plane are well known, and their expressions can be found, for instance, in Ting's book [29]. For an anisotropic half-plane, the Green's functions were studied by Suo [11] using the one-complex function method, and by Ting [29] based on the Stroh formalism. Using the one-complex function method, the authors derived the *complete* Green's functions and incorporated them into their anisotropic half-plane BEM formulation [30].

Green's functions in anisotropic and elastic bimaterials were studied previously by Tewary et al. [10] using the Fourier transform method, by Suo [11] using the one-complex function method, and by Ting [29] using the Stroh formalism. Recently, the first author, [31] derived the *complete* Green's functions for anisotropic piezoelectric infinite plane, half plane and two joined dissimilar half planes. In the following we present briefly the Green's function solution for a point force in an anisotropic and elastic bimaterial. The procedure is similar to that used by Suo [11] and Pan [31].

With three complex analytical functions $f_i(z_i)$, one can, in general, express displacements, stresses, and tractions as follows [11,26,29]

$$u_i = 2\mathrm{Re}[\sum_{i=1}^{3} A_{ij} f_j(z_j)] \qquad \sigma_{2i} = 2\mathrm{Re}[\sum_{j=1}^{3} B_{ij} f'_j(z_j)]$$
$$\sigma_{1i} = -2\mathrm{Re}[\sum_{i=1}^{3} B_{ij}\mu_j f'_j(z_j)] \qquad T_i = -2\mathrm{Re}[\sum_{j=1}^{3} B_{ij} f_j(z_j)] \tag{1}$$

where $z_j = x + \mu_j y$; Re denotes the real part of a complex variable or function; a prime denotes the derivative; the three complex number $\mu_j (j = 1, 2, 3)$ and the elements of the complex matrices **B** and **A** are functions of the elastic properties [11,26,29].

Assume that the medium is composed of two joined dissimilar anisotropic and elastic half-planes. We let the interface be along the x-axis, and the upper ($y > 0$) and lower ($y < 0$) half-planes be occupied by materials #1 and #2, respectively.

For concentrated force acting at the point (x^0, y^0) in material #2 ($y^0 < 0$), we express the complex vector function as [11]

$$f(z) = \begin{cases} f^{\mathrm{U}}(z) & z \in 1 \\ f^{\mathrm{L}}(z) + f^0_{(2)}(z) & z \in 2 \end{cases} \tag{2}$$

where the vector function

$$f(z) = [f_1(z), f_2(z), f_3(z)]^{\mathrm{T}} \tag{3}$$

with the argument having the generic form $z = x + \mu y$.

In Eq. (2), $f^0_{(2)}$ is a singular solution corresponding to a point force acting at the point (x^0, y^0) in an anisotropic infinite plane with the elastic properties of material #2. This singular solution can be expressed as [11,29]

$$f_j(z) = \frac{-1}{2\pi} \{\mathbf{Hp}\}_j \ln(z - s_j) \tag{4}$$

where $s_j = x^0 + \mu_j y^0$, **p** is the point force vector, and **H** is given by

$$\mathbf{H} = \mathbf{A}^{-1}(\mathbf{Y}^{-1} + \bar{\mathbf{Y}}^{-1})^{-1}; \quad \mathbf{Y} = i\mathbf{A}\mathbf{B}^{-1} \tag{5}$$

There are two unknown vector functions to be solved in Eq. (2), that is $\mathbf{f}^{\mathrm{U}}(z)$ and $\mathbf{f}^{\mathrm{L}}(z)$. While the former is analytic in the upper (material #1) half plane, the latter is analytic in the lower (material #2) half-plane. These expressions can be found by requiring continuity of the resultant traction and displacement across the interface, along with the standard analytic continuation arguments. Following this approach and after some complex algebraic manipulation, the complex vector functions in materials #1 and #2 are obtained as

$$\mathbf{f}(z) = \begin{cases} \mathbf{B}^{-1}_{(1)}(\mathbf{Y}_{(1)} + \bar{\mathbf{Y}}_{(2)})^{-1}(\bar{\mathbf{Y}}_{(2)} + \mathbf{Y}_{(2)})\mathbf{B}_{(2)}\mathbf{f}^0_{(2)}(z) & z \in 1 \\ \mathbf{B}^{-1}_{(2)}(\bar{\mathbf{Y}}_{(1)} + \mathbf{Y}_{(2)})^{-1}(\bar{\mathbf{Y}}_{(2)} - \bar{\mathbf{Y}}_{(1)})\bar{\mathbf{B}}_{(2)}\bar{\mathbf{f}}^0_{(2)}(z) + \mathbf{f}^0_{(2)}(z) & z \in 2 \end{cases}. \tag{6}$$

In Eq. (6), the special subscript (1) and (2) are used exclusively to denote that the corresponding matrix or vector is in material #1 ($y > 0$) and material #2 ($y < 0$), respectively.

Similarly, for a point force in material #1 ($y^0 > 0$), these complex functions can be found as

$$\mathbf{f}(z) = \begin{cases} \mathbf{B}_{(1)}^{-1}(\bar{\mathbf{Y}}_{(2)} + \mathbf{Y}_{(1)})^{-1}(\bar{\mathbf{Y}}_{(1)} - \bar{\mathbf{Y}}_{(2)})\bar{\mathbf{B}}_{(1)}\bar{\mathbf{f}}_{(1)}^{0}(z) + \mathbf{f}_{(1)}^{0}(z) & z \in 1 \\ \mathbf{B}_{(2)}^{-1}(\mathbf{Y}_{(2)} + \bar{\mathbf{Y}}_{(1)})^{-1}(\bar{\mathbf{Y}}_{(1)} + \mathbf{Y}_{(1)})\mathbf{B}_{(1)}\mathbf{f}_{(1)}^{0}(z) & z \in 2 \end{cases} \tag{7}$$

where the vector functions $\mathbf{f}_{(1)}^{0}$ is the infinite-plane solution given in Eq. (4) but with the elastic properties of material #1.

With the complex functions given in Eqs. (6) and (7), the Green's functions of the displacement and traction can be obtained by substituting these complex functions into Eq. (1). These Green's functions have four different forms depending on the relative locations of the field and source points. Their complete expressions are given in Appendix A.

It is noteworthy that these Green's functions can be used to solve both plane stress and plane strain problems in anisotropic bimaterials. Although the isotropic solution cannot be analytically reduced from these Green's functions, one can numerically approximate it by selecting a very weak anisotropic (or nearly isotropic) medium [24,32].

3. BEM formulation for 2D cracked anisotropic bimaterials

It is well known that a cracked domain poses certain difficulties for BEM modeling [33]. Previously, fracture mechanics problems in isotropic or anisotropic bimaterials were mostly handled by the multi-domain method in which each side of the crack surface is put into different domains and artificial boundaries are introduced to connect the crack surface to the uncracked boundary. For the bimaterial case, discretization along the interface is also required if one uses the Kelvin-type (infinite domain) Green's functions.

In this section, we present a single-domain BEM formulation in which neither the artificial boundary nor the discretization along the uncracked interface is necessary. This single-domain BEM formulation was widely used recently [23,34] for homogeneous materials and is now extended to anisotropic bimaterials.

For a point $\mathbf{P}_s$ on the uncracked boundary, the following displacement integral equation can be derived [24]

$$\begin{aligned} & b_{ij}u_j^{\mathrm{t}}(\mathbf{P}_s) + \int_s T_{ij}^{*}(\mathbf{P}_s, \mathbf{X}_s)u_j^{\mathrm{t}}(\mathbf{X}_s)\,\mathrm{d}S(\mathbf{X}_s) + \int_{\Gamma} T_{ij}^{*}(\mathbf{P}_s, \mathbf{X}_{\Gamma+}) \\ & \quad \times [u_j^{\mathrm{t}}(\mathbf{X}_{\Gamma+}) - u_j^{\mathrm{t}}(\mathbf{X}_{\Gamma-})]\,\mathrm{d}\Gamma(\mathbf{X}_{\Gamma+}) \\ & = \int_s U_{ij}^{*}(\mathbf{P}_s, \mathbf{X}_s)T_j^{\mathrm{t}}(\mathbf{X}_s)\,\mathrm{d}S(\mathbf{X}_s) + \int_s T_{ij}^{*}(\mathbf{P}_s, \mathbf{X}_s)(u_j^{\mathrm{p}}(\mathbf{X}_s) \\ & \quad - u_i^{\mathrm{p}}(\mathbf{P}_s))\,\mathrm{d}S(\mathbf{X}_s) \\ & \quad - \int_s U_{ij}^{*}(\mathbf{P}_s, \mathbf{X}_s)T_j^{\mathrm{p}}(\mathbf{X}_s)\,\mathrm{d}S(\mathbf{X}_s) \end{aligned} \tag{8}$$

where the superscripts t and p denote the total and particular solutions, respectively; b_{ij} are coefficients that depend only upon the local geometry of the uncracked boundary at $\mathbf{P}_s$; $\mathrm{d}S$ and $\mathrm{d}\Gamma$ are the line elements on the uncracked boundary and crack surface, respectively, with the corresponding points being denoted by subscript s and Γ; U_{ij}^{*} and T_{ij}^{*} are the bimaterial Green's displacements and tractions given in Appendix A; and a point on the positive (or negative) side of a crack is denoted by $\mathbf{X}_{\Gamma+}$ (or $\mathbf{X}_{\Gamma-}$). In deriving Eq. (8), we have assumed that the tractions on the two faces of a crack are equal and opposite. We emphasize here that since the bimaterial Green's functions are included in Eq. (8), discretization along the interface can be avoided, with the exception of the interfacial crack part which will be treated by the traction integral equation presented below.

It is noted that all the terms on the right-hand side of Eq. (8) have only weak singularities, thus, are integrable. Although the second term on the left-hand side of Eq. (8) has a strong singularity, it can be treated by the rigid-body motion method. At the same time, the calculation of b_{ij}, which is geometry dependent, can also be avoided.

Since, for a cracked domain, Eq. (8) does not have a unique solution for the unknowns [23,33,34], we introduce a traction integral equation [25] for the anisotropic medium. Assume that $\mathbf{P}_{\Gamma}$ is a smooth point on the crack, the traction

Table 1
Comparison of the SIFs (horizontal crack)

G_2/G_1	$d/2a$	$K_I/p\sqrt{\pi a}$			$K_{II}/p\sqrt{\pi a}$		
		Isida and Noguchi [37]	Yuuki and Cho [17]	Present	Isida and Noguchi [37]	Yuuki and Cho [17]	Present
0.25	0.05	1.468	1.4684	1.4773	0.286	0.2923	0.2862
0.25	0.5	1.197	1.1964	1.1982	0.071	0.0717	0.0706
2.0	0.05	0.872	0.8693	0.8712	−0.087	−0.0848	−0.0869
2.0	0.5	0.935	0.9341	0.9354	−0.024	−0.0226	−0.0235

integral equation can be derived as

$$
\begin{aligned}
&0.5[T_l^{\mathrm{t}}(\mathbf{P}_{\Gamma+}) - T_l^{t}(\mathbf{P}_{\Gamma-})] \\
&\quad + n_{\mathrm{m}}(\mathbf{P}_{\Gamma+}) \int_s c_{\mathrm{lmik}} T^*_{ij,k}(\mathbf{P}_{\Gamma+}, \mathbf{X}_{\mathrm{s}}) u_j^{\mathrm{t}}(\mathbf{X}_{\mathrm{s}})\, \mathrm{d}S(\mathbf{X}_{\mathrm{s}}) \\
&\quad + n_{\mathrm{m}}(\mathbf{P}_{\Gamma+}) \int_{\Gamma} c_{\mathrm{lmik}} T^*_{ij,k}(\mathbf{P}_{\Gamma+}, \mathbf{X}_{\Gamma+}) [u_j^{\mathrm{t}}(\mathbf{X}_{\Gamma+}) \\
&\quad - u_j^{\mathrm{t}}(\mathbf{X}_{\Gamma-})]\, \mathrm{d}\Gamma(\mathbf{X}_{\Gamma+}) \\
&= 0.5[T_l^{\mathrm{p}}(\mathbf{P}_{\Gamma+}) - T_l^{\mathrm{p}}(\mathbf{P}_{\Gamma-})] \\
&\quad + n_{\mathrm{m}}(\mathbf{P}_{\Gamma+}) \int_s c_{\mathrm{lmik}} U^*_{ij,k}(\mathbf{P}_{\Gamma+}, \mathbf{X}_{\mathrm{s}}) T_j^{\mathrm{t}}(\mathbf{X}_{\mathrm{s}})\, \mathrm{d}S(\mathbf{X}_{\mathrm{s}}) \\
&\quad + n_{\mathrm{m}}(\mathbf{P}_{\Gamma+}) \int_s c_{\mathrm{lmik}} T^*_{ij,k}(\mathbf{P}_{\Gamma+}, \mathbf{X}_{s}) u_j^{\mathrm{p}}(\mathbf{X}_{s})\, \mathrm{d}S(\mathbf{X}_{s}) \\
&\quad - n_{\mathrm{m}}(\mathbf{P}_{\Gamma+}) \int_s c_{\mathrm{lmik}} U^*_{ij,k}(\mathbf{P}_{\Gamma+}, \mathbf{X}_{s}) T_j^{\mathrm{p}}(\mathbf{X}_{s})\, \mathrm{d}S(\mathbf{X}_{s})
\end{aligned}
\tag{9}
$$

where n_{m} is the outward normal at the crack surface $P_{\Gamma+}$ and c_{lmik} is the fourth order stiffness tensor.

Eqs. (8) and (9) form a pair of boundary integral equations [23,25,35] and can be used for the calculation of SIFs in anisotropic bimaterials. The main feature of this BEM formulation is that it is a single-domain formulation with the displacement integral Eq. (8) being collocated on the uncracked boundary only and the traction integral Eq. (9) on one side of the crack surface only. For problems without cracks, one needs Eq. (8) only, with the integral on the crack surface being discarded. Eq. (8) then reduces to the well-known displacement integral equation. On the other hand, for problems containing crack surface only, one needs Eq. (9) only, with the integral on the uncracked boundary being discarded. Eq. (9) then reduces to the well-known DDM formulation [35].

For given particular solutions (related to the body force of gravity, rotational forces, and the far-field stresses), the boundary integral equations (8) and (9) can be discretized and solved numerically for the unknown boundary displacements (or displacement discontinuities on the crack surface) and tractions. In solving these equations, the hypersingular integral term involved in Eq. (9) can be handled by an accurate and efficient Gauss quadrature formulae which is similar to the traditional weighted Gauss quadrature but with a different weight [24,36].

4. Crack-tip modelling

In fracture mechanics analysis, especially in the calculation of the SIFs, one needs to know the asymptotic behavior of the displacements and stresses near the crack-tip. In our BEM analysis of the SIFs, we propose to use the extrapolation method of the crack-tip displacements. We therefore need to know the exact asymptotic behavior of the relative crack displacements behind the crack-tip. This asymptotic expression has different forms depending on the location of the crack-tip. In this paper, two cases will be discussed, that is, a crack-tip within the homogeneous material and an interfacial crack-tip. Inclined cracks terminated at the interface will be discussed in a future paper.

4.1. A crack-tip within a homogeneous material

Assume that the crack-tip is within material #1, the asymptotic behavior of the relative displacement at a distance r behind the crack-tip can be expressed in terms of the three SIFs as [11]:

$$\Delta\mathbf{u}(r) = 2\sqrt{\frac{2r}{\pi}}\,\mathrm{Re}(\mathbf{Y}_{(1)})\mathbf{K} \tag{10}$$

where

$$\mathbf{K} = [K_{II}, K_I, K_{III}]^{\mathrm{T}} \tag{11}$$

is the SIF vector, and $\mathbf{Y}$ is a matrix with elements related to the anisotropic properties in material #1, as defined in Eq. (5).

In order to capture the square-root characteristics of the relative crack open displacements (COD) near the crack-tip, we construct the following new crack-tip element with the tip at $s = -1$:

$$\Delta u_i = \sum_{k=1}^{3} \phi_k \Delta u_i^k \tag{12}$$

where the subscript i denotes the relative COD component and the superscript $k(= 1, 2, 3)$ denotes the relative CODs at nodes $s = -2/3, 0, 2/3$, respectively. The shape functions ϕ_k are those introduced by Pan [25]

$$
\begin{aligned}
\phi_1 &= \tfrac{3\sqrt{3}}{8}\sqrt{s+1}[5 - 8(s+1) + 3(s+1)^2] \\
\phi_2 &= \tfrac{1}{4}\sqrt{s+1}[-5 + 18(s+1) - 9(s+1)^2] \\
\phi_3 &= \tfrac{3\sqrt{3}}{8\sqrt{5}}\sqrt{s+1}[1 - 4(s+1) + 3(s+1)^2]
\end{aligned}
\tag{13}
$$

The node displacements in Eq. (12) are obtained in solving the discretized formulations of the boundary integral equations (8) and (9). Equating these displacements to those given in Eq. (10) and extrapolating to the crack-tip gives the SIFs.

4.2. An interfacial crack-tip

For this case, the relative crack displacements at a distance r behind the interfacial crack-tip can be expressed, in terms of the three SIFs, as [16]

$$\Delta\mathbf{u}(r) = \Big(\sum_{j=1}^{3} c_j \mathbf{D}\mathbf{Q}_j\, \mathrm{e}^{-\pi\delta_j} r^{1/2+i\delta_j}\Big)\mathbf{K} \tag{14}$$

with c_j, δ_j, $\mathbf{Q}_{\mathrm{j}}$ and $\mathbf{D}$ being defined in Appendix B. Comparing this equation to Eq. (10), we notice that while the

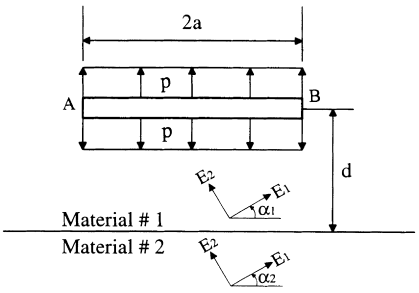

Fig. 1. A horizontal crack under uniform pressure within material #1 of an infinite bimaterials.

relative crack displacement behaves as a square-root for a crack-tip within a homogeneous medium, for an interfacial crack-tip, its behavior is $r^{1/2+i\delta}$, a square-root feature multiplied by weak oscillatory behaviors.

Eq. (14) can be recast into the following form, which is more convenient for the current numerical applications:

$$\Delta\mathbf{u}(r) = \sqrt{\frac{2r}{\pi}}\mathbf{M}\left(\frac{r}{d}\right)\mathbf{K} \tag{15}$$

where d is the characteristic length, and $\mathbf{M}$ is a matrix function with its expression being given in Appendix B.

Again, in order to capture the square-root and the weak oscillatory behavior, we construct a crack-tip element with tip at $s = -1$ in terms of which the relative crack displacement is expressed as

$$\Delta\mathbf{u}(r) = \mathbf{M}\left(\frac{r}{d}\right)\begin{bmatrix} \phi_1\Delta u_1^1 + \phi_2\Delta u_1^2 + \phi_3\Delta u_1^3 \\ \phi_1\Delta u_2^1 + \phi_2\Delta u_2^2 + \phi_3\Delta u_2^3 \\ \phi_1\Delta u_3^1 + \phi_2\Delta u_3^2 + \phi_3\Delta u_3^3 \end{bmatrix} \tag{16}$$

It is noted that this expression of the interfacial crack-tip displacement is similar to that proposed by Tan et al. [19]. Once the nodal displacements in Eq. (16) are solved, the interfacial SIFs can then be obtained by equating the relative displacements in equation (16) to those in Eq. (15), and by extrapolating to the crack-tip.

5. Numerical examples

The aforementioned Green's functions and the particular crack-tip elements have been incorporated into the boundary integral equations presented above, and the results have been programmed. In this section, three numerical examples are presented to verify the formulation and to show the efficiency and versatility of the present BEM method for problems related to fracture in anisotropic bimaterial full-space.

Example 1. Horizontal crack in material #1

A horizontal crack under a uniform pressure p is shown in Fig. 1. The crack has a length, $2a$, and is located at a distance, d, to the interface. The Poisson ratios for both materials #1 and 2 are the same, i.e. $\nu_1 = \nu_2 = 0.3$, while the ratio of the shear moduli G_2/G_1 varies. A plane stress condition is assumed. In order to calculate the SIFs at the crack tip A or B, 20 quadratic elements were used to discretize the crack surface. The results are given in Table 1 for various values of the shear moduli ratio. They are compared to the results given by Isida and Noguchi [37] using a body-force integral equation method and those by Yuuki and Cho [17] using a multi-domain BEM formulation. As can be observed from this table, the results compare quite well.

The mode III SIF was also calculated when the crack surface is loaded by a uniform anti-shear stress q. The SIFs calculated by the present method are: $K_{III}/q\sqrt{\pi a} = 1.3648$ and 1.0534 for $d/2a = 0.05$ and 0.5, respectively when $G_2/G_1 = 0.25$; and $K_{III}/q\sqrt{\pi a} = 0.8927$ and 0.9739 for $d/2a = 0.05$ and 0.5, respectively, when $G_2/G_1 = 2.0$.

The effect of material anisotropy on the SIFs was also studied for this example. The anisotropic elastic properties in material #1 were assumed to be those of glass/epoxy with $E_1 = 48.26$ GPa, $E_2 = 17.24$ GPa, $G_{12} = 6.89$ GPa, $\nu_{12} = 0.29$. For material #2, a graphite/epoxy with $E_1 = 144.8$ GPa, $E_2 = 11.7$ GPa, $G_{12} = 9.66$ GPa, $\nu_{12} = 0.21$ was selected [38]. The material axis E_1 in materials #1 and #2 makes angles α_1 and α_2, respectively, with respect to the horizontal direction (Fig. 1).

Figs. 2–4 show the variation of the SIFs at tips A and B with the angle α_2 as it varies between 0 and 90°. In these figures, α_1 is 0, 45 and 90°, respectively. These figures show that while K_1 decreases with increasing α_2, K_{II} reaches a minimum between $\alpha_2 = 0$ and $\alpha_2 = 90$.

Example 2. Vertical crack intersecting an interface

Consider a vertical crack intersecting an interface and subjected to far-field horizontal stresses as shown in Fig. 5. The horizontal far field stresses applied in materials #1 and #2 are, respectively, σ_1 and σ_2 $(= \sigma_1 G_2/G_1)$. The Poisson ratios ν_1 and ν_2 are again assumed to be equal to 0.3 and the shear modulus ratio G_2/G_1 is assumed to vary. The distance of the crack tips A and B to the interface are the same, i.e. $d_1 = d_2 = a$, the half-length of the crack. Again, a plane stress condition is assumed and 20 quadratic elements were used to discretize the crack surface. The SIFs at the crack tips A and B are listed in Table 2 for several values of the shear modulus ratio, and are compared to those given by Isida and Noguchi [37]. Again, the results between the two numerical analyses compare quite well.

Example 3. Interfacial horizontal crack in infinite bimaterials

An interfacial crack along the x-axis of length $2a$ is shown in Fig. 6. The crack surface is under a uniform pressure p and the materials can be either isotropic or anisotropic. Twenty quadratic elements were used to discretize the crack and the characteristic length is assumed as $2a$.

The normalized SIFs under plane stress condition are

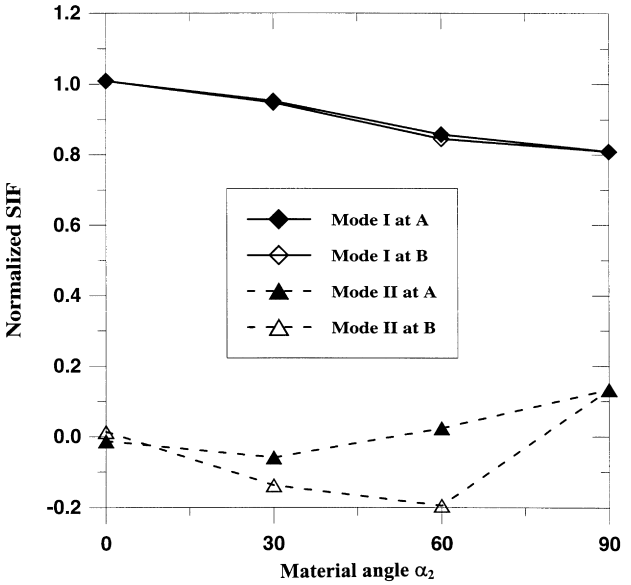

Fig. 2. Variation of the SIFs at crack tips A and B of Fig. 1 with material angle α_2 when material angle $\alpha_1 = 0°$.

listed in Table 3 for various values of the shear modulus ratio G_1/G_2 (with $\nu_1 = \nu_2 = 0.3$), and are compared to the exact solution proposed by Rice [4]. A very good agreement is found between the numerical analysis and the exact solution.

The SIFs at the crack tips of an interfacial crack were also calculated for the anisotropic bimaterial case. The anisotropic elastic properties in materials #1 and #2 are the same as those in Example 1. While the material axis E_1 in material #2 was assumed to be along the horizontal direction (i.e. $\alpha_2 = 0$), the E_1-axis in material #1 makes an angle α_1 with respect to the horizontal direction. The interfacial SIFs at crack tip B obtained by the present method are listed in Table 4 and compared to the exact solutions proposed by Wu [12]. Table 5 lists the results when the E_1-axis in material #1 is along the horizontal direction ($\alpha_1 = 0$) and the E_1-axis in material #2 makes an angle α_2 with respect to the horizontal direction. Tables 4 and 5 indicate that the present method can also be used to calculate accurately the interfacial SIFs.

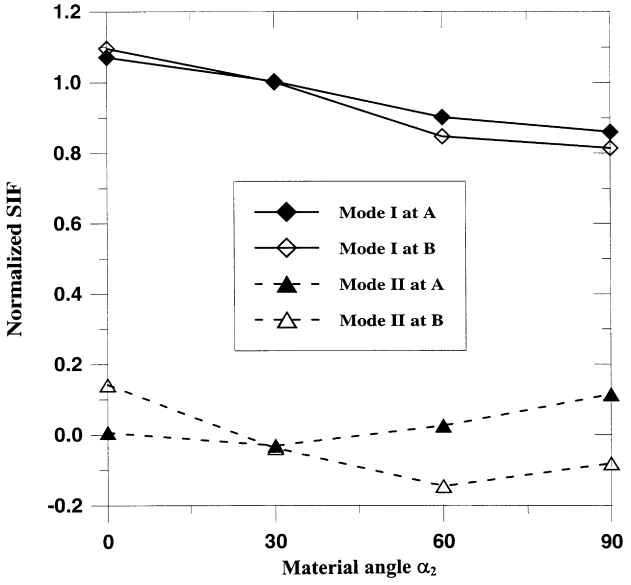

Fig. 3. Same as in Fig. 2, but with material angle $\alpha_1 = 45°$.

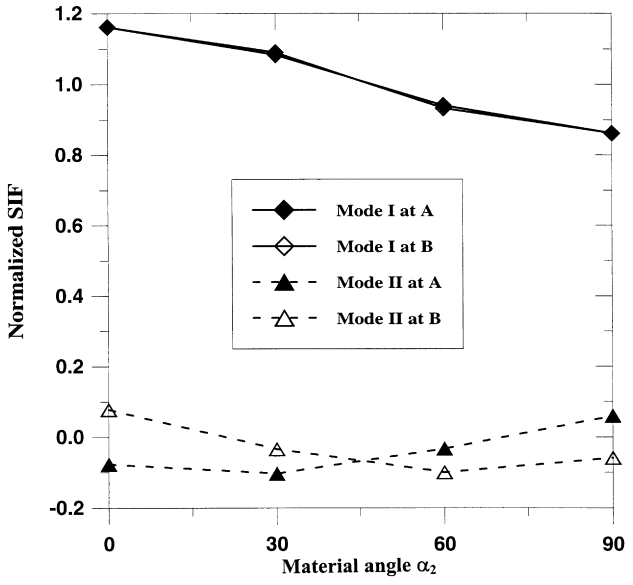

Fig. 4. Same as in Fig. 2, but with material angle $\alpha_1 = 90°$.

6. Conclusions

A BEM formulation has been proposed for fracture mechanics analysis of cracked 2D anisotropic elastic bimaterials in which the displacement and traction integral equations are collocated on the outside boundary (uncracked boundary) only and on one side of the crack surface only, respectively. Since in the present BEM formulation, the displacements or tractions are used as unknowns on the outside boundary and displacement differences as unknowns along the crack surface, the method proposed herein combines the best attributes of the traditional displacement BEM and the DDM. While the Cauchy singularity in the displacement equation is avoided by the common rigid-body motion method, the hyper-singularity in the traction

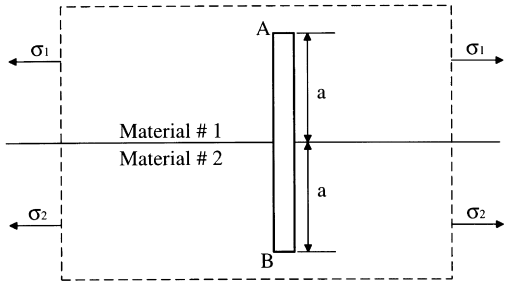

Fig. 5. Vertical crack intersecting an interface under far-field stresses.

Table 2
Comparison of the SIFs (vertical crack)

G_2/G_1	Isida and Noguchi [37]		Present	
	$K_I^A/\sigma_1\sqrt{\pi a}$	$K_I^B/\sigma_2\sqrt{\pi a}$	$K_I^A/\sigma_1\sqrt{\pi a}$	$K_I^B/\sigma_2\sqrt{\pi a}$
0.1	1.062	1.153	1.063	1.156
0.3	1.015	1.064	1.016	1.066
0.5	1.000	1.028	1.001	1.029
0.8	0.997	1.006	0.998	1.007

Table 3
Comparison of the SIFs for isotropic case (interfacial crack)

G_1/G_2	Exact [4]		Numerical	
	$K_I/p\sqrt{\pi a}$	$K_{II}/p\sqrt{\pi a}$	$K_I/p\sqrt{\pi a}$	$K_{II}/p\sqrt{\pi a}$
2.0	1.0000	0.0746	1.0038	0.0747
3.0	1.0000	0.1126	1.0055	0.1122
4.0	1.0000	0.1357	0.9999	0.1347
5.0	1.0000	0.1513	0.9986	0.1497
10.0	1.0000	0.1875	0.9954	0.1839
100.0	1.0000	0.2276	0.9917	0.2206

Table 4
Comparison of the SIFs for anisotropic case $\alpha_2 = 0^\circ$ (interfacial crack)

α_1	Exact [12]		Numerical	
	$K_I/p\sqrt{\pi a}$	$K_{II}/p\sqrt{\pi a}$	$K_I/p\sqrt{\pi a}$	$K_{II}/p\sqrt{\pi a}$
0	1.0000	− 0.0382	1.0054	− 0.0384
30	0.9968	− 0.0349	1.0022	− 0.0351
45	0.9965	− 0.0318	1.0019	− 0.0320
60	0.9971	− 0.0290	1.0025	− 0.0291
90	1.0000	− 0.0264	1.0054	− 0.0265

Table 5
Comparison of the SIFs for anisotropic case $\alpha_1 = 0^\circ$ (interfacial crack)

α_2	Exact [12]		Numerical	
	$K_I/p\sqrt{\pi a}$	$K_{II}/p\sqrt{\pi a}$	$K_I/p\sqrt{\pi a}$	$K_{II}/p\sqrt{\pi a}$
0	1.0000	− 0.0383	1.0054	− 0.0384
30	0.9941	− 0.0334	0.9995	− 0.0335
45	0.9936	− 0.0289	0.9989	− 0.0290
60	0.9946	− 0.0247	1.0000	− 0.0248
90	1.0000	− 0.0208	1.0054	− 0.0209

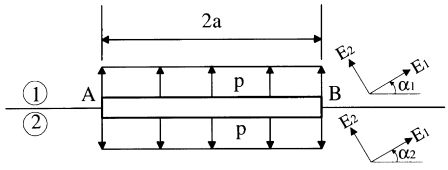

Fig. 6. Interfacial crack within infinite bimaterials.

equation is handled by introducing a new Gauss quadrature formulae which is very similar to the traditional weighted Gauss quadrature but with a different weight.

Three numerical examples related to a crack in an infinite bimaterial full-space were selected to show that with the current BEM formulation, very accurate SIFs can be obtained. These examples also show the effect of material anisotropy on the SIFs. Since the present method is simple and can be used for curved cracks, it will be straightforward to extend the current BEM formulation to analyze fracture propagation in 2D anisotropic bimaterials, which is currently under investigation by the authors.

Acknowledgements

The authors are grateful for the support of National Science Foundation under Grant CMS-9713559 and Air Force Office of Scientific Research under Grant F49620-98-1-0104. They also like to thank one of the reviewers for the helpful comments.

Appendix A. Complete Green's functions for anisotropic elastic bimaterials

In this appendix, we present the complete Green's functions for the displacement U_{kl}^* and traction T_{kl}^*. Special superscripts and subscripts (1) and (2) are used exclusively to denote that the corresponding quantities are in materials #1 ($y > 0$) and #2 ($y < 0$), respectively.

A.1. For source (s) and field (z) points in materials #1 ($y > 0$)

$$U_{kl}^* = \frac{-1}{\pi}\mathrm{Re}\{\sum_{j=1}^{3} A_{lj}^{(1)}[\ln(z_j^{(1)} - s_j^{(1)})H_{jk}^{(1)} + \sum_{i=1}^{3} W_{ji}^{11}\ln(z_j^{(1)} - \bar{s}_i^{(1)})\bar{H}_{ik}^{(1)}]\} \tag{A1}$$

$$T_{kl}^* = \frac{1}{\pi}\mathrm{Re}\left\{\sum_{j=1}^{3} B_{lj}^{(1)}\left[\frac{\mu_j^{(1)}n_x - n_y}{z_j^{(1)} - s_j^{(1)}}H_{jk}^{(1)} + \sum_{i=1}^{3} W_{ji}^{11}\frac{\mu_j^{(1)}n_x - n_y}{z_j^{(1)} - \bar{s}_i^{(1)}}\bar{H}_{ik}^{(1)}\right]\right\} \tag{A2}$$

where the matrix $\mathbf{H}$ is defined in Eq. (5) with the anisotropic elastic properties of material #1, and

$$\mathbf{W}^{11} = \mathbf{B}_{(1)}^{-1}(\mathbf{Y}_{(1)} + \bar{\mathbf{Y}}_{(2)})^{-1}(\bar{\mathbf{Y}}_{(1)} - \bar{\mathbf{Y}}_{(2)})\bar{\mathbf{B}}_{(1)} \tag{A3}$$

A.2. For source point (s) in material #1 ($y > 0$) and field point (z) in material #2 ($y < 0$)

$$U_{kl}^{*} = \frac{-1}{\pi}\mathrm{Re}\{\sum_{j=1}^{3} A_{lj}^{(2)}[\sum_{i=1}^{3} W_{ji}^{12}\ln(z_j^{(2)} - s_i^{(1)})H_{ik}^{(1)}]\} \tag{A4}$$

$$T_{kl}^{*} = \frac{1}{\pi}\mathrm{Re}\left\{\sum_{j=1}^{3} B_{lj}^{(2)}\left[\sum_{i=1}^{3} W_{ji}^{12}\frac{\mu_j^{(2)}n_x - n_y}{z_j^{(2)} - s_i^{(1)}}H_{ik}^{(1)}\right]\right\} \tag{A5}$$

with

$$\mathbf{W}^{12} = \mathbf{B}_{(2)}^{-1}(\mathbf{Y}_{(2)} + \bar{\mathbf{Y}}_{(1)})^{-1}(\bar{\mathbf{Y}}_{(1)} + \mathbf{Y}_{(1)})\mathbf{B}_{(1)} \tag{A6}$$

A.3. For source (s) and field (z) points in material #2 ($y < 0$)

$$U_{kl}^{*} = \frac{-1}{\pi}\mathrm{Re}\{\sum_{j=1}^{3} A_{lj}^{(2)}[\ln(z_j^{(2)} - s_j^{(2)})H_{jk}^{(2)} + \sum_{i=1}^{3} W_{ji}^{22}\ln(z_j^{(2)} - \bar{s}_i^{(2)})\bar{H}_{ik}^{(2)}]\} \tag{A7}$$

$$T_{kl}^{*} = \frac{1}{\pi}\mathrm{Re}\left\{\sum_{j=1}^{3} B_{lj}^{(2)}\left[\frac{\mu_j^{(2)}n_x - n_y}{z_j^{(2)} - s_j^{(2)}}H_{jk}^{(2)} + \sum_{i=1}^{3} W_{ji}^{22}\frac{\mu_j^{(2)}n_x - n_y}{z_j^{(2)} - \bar{s}_i^{(2)}}\bar{H}_{ik}^{(2)}\right]\right\} \tag{A8}$$

where the matrix $\mathbf{H}$ is defined in Eq. (5) with the anisotropic material properties of material #2, and

$$\mathbf{W}^{22} = \mathbf{B}_{(2)}^{-1}(\mathbf{Y}_{(2)} + \bar{\mathbf{Y}}_{(1)})^{-1}(\bar{\mathbf{Y}}_{(2)} - \bar{\mathbf{Y}}_{(1)})\bar{\mathbf{B}}_{(2)} \tag{A9}$$

A.4. For source point (s) in material #2 ($y < 0$) and field point (z) in material #1 ($y > 0$)

$$U_{kl}^{*} = \frac{-1}{\pi}\mathrm{Re}\{\sum_{j=1}^{3} A_{lj}^{(1)}[\sum_{i=1}^{3} W_{ji}^{21}\ln(z_j^{(1)} - s_i^{(2)})H_{ik}^{(2)}]\} \tag{A10}$$

$$T_{kl}^{*} = \frac{1}{\pi}\mathrm{Re}\left\{\sum_{j=1}^{3} B_{lj}^{(1)}\left[\sum_{i=1}^{3} W_{ji}^{21}\frac{\mu_j^{(1)}n_x - n_y}{z_j^{(1)} - s_i^{(2)}}H_{ik}^{(2)}\right]\right\} \tag{A11}$$

with

$$\mathbf{W}^{21} = \mathbf{B}_{(1)}^{-1}(\mathbf{Y}_{(1)} + \bar{\mathbf{Y}}_{(2)})^{-1}(\bar{\mathbf{Y}}_{(2)} + \mathbf{Y}_{(2)})\mathbf{B}_{(2)} \tag{A12}$$

Appendix B. Asymptotic expressions of displacements at an interfacial crack-tip

The derivative of the interfacial crack displacements follows that of Gao et al.[16]. The relative displacement vector on the crack face was given by Eq. (14) in which

$$c_1 = \frac{2}{\sqrt{2\pi}\beta^2};\ c_2 = \frac{-\mathrm{e}^{-\pi\varepsilon}d^{i\varepsilon}}{\sqrt{2\pi}(1 + 2i\varepsilon)\beta^2\cosh(\pi\varepsilon)};$$
$$c_3 = \frac{-\mathrm{e}^{\pi\varepsilon}d^{i\varepsilon}}{\sqrt{2\pi}(1 - 2i\varepsilon)\beta^2\cosh(\pi\varepsilon)} \tag{B1}$$

$$\beta = \sqrt{-\frac{1}{2}tr(\mathbf{P}^2)} \tag{B2}$$

$$\varepsilon = \frac{1}{2\pi}\ln\frac{1+\beta}{1-\beta} = \frac{1}{\pi}\tanh^{-1}\beta \tag{B3}$$

$$\delta_1 = 0;\ \delta_2 = \varepsilon;\ \delta_3 = -\varepsilon \tag{B4}$$

$$\mathbf{Q}_1 = \mathbf{P}^2 + \beta^2\mathbf{I};\ \mathbf{Q}_2 = \mathbf{P}(\mathbf{P} - i\beta\mathbf{I});\ \mathbf{Q}_3 = \mathbf{P}(\mathbf{P} + i\beta\mathbf{I}) \tag{B5}$$

where $\mathbf{I}$ is a 3×3 identity matrix. In Eqs. (B2) and (B5), the matrix $\mathbf{P}$ is given by

$$\mathbf{P} = -\mathbf{D}^{-1}\mathbf{V} \tag{B6}$$

where $\mathbf{D}$ and $\mathbf{V}$ are two real matrices obtained from the following relation:

$$\mathbf{Y}_{(1)} + \bar{\mathbf{Y}}_{(2)} = \mathbf{D} - i\mathbf{V} \tag{B7}$$

In Eq. (16), the matrix function is given by

$$\mathbf{M}(x) = \frac{\mathbf{D}}{\beta^2}\left\{(\mathbf{P}^2 + \beta^2\mathbf{I}) - \frac{[\cos(\varepsilon\ln x) + 2\varepsilon\sin(\varepsilon\ln x)]\mathbf{P}^2 + \beta[\sin(\varepsilon\ln x) - 2\varepsilon\cos(\varepsilon\ln x)]\mathbf{P}}{(1 + 4\varepsilon^2)\cosh(\pi\varepsilon)}\right\} \tag{B8}$$

References

[1] Williams ML. The stresses around a fault or crack in dissimilar media. Bull Seism Soc Am 1959;49:199–204.
[2] England AH. A crack between dissimilar media. J Appl Mech 1965;32:400–2.
[3] Rice JR, Sih G. Plane problems of cracks in dissimilar media. J Appl Mech 1965;32:418–23.
[4] Rice JR. Elastic fracture mechanics concepts for interfacial cracks. J Appl Mech 1988;55:98–103.
[5] Clements DL. A crack between dissimilar anisotropic media. Int J Engng Sci 1971;9:257–65.
[6] Willis JR. Fracture mechanics of interfacial cracks. J Mech Phys Solids 1971;19:353–68.
[7] Ting TCT. Explicit solution and invariance of the singularities at an interface crack in anisotropic composites. Int J Solids Structures 1986;22:965–83.
[8] Ting TCT. Interface cracks in anisotropic bimaterials. J Mech Phys Solids 1990;38:505–13.
[9] Bassani JL, Qu J. Finite cracks on bimaterial and bicrystal interfaces. J Mech Phys Solids 1989;37:435–53.
[10] Tewary VK, Wagoner RH, Hirth JP. Elastic Green's function for a composite solid with a planar interface. J Mater Res 1989;4:113–23.

[11] Suo Z. Singularities, interfaces and cracks in dissimilar anisotropic media. Proc R Soc Lond A 1990;427:331–58.
[12] Wu KC. Stress intensity factor and energy release rate for interfacial cracks between dissimilar anisotropic materials. J Appl Mech 1990;57:882–6.
[13] Wu KC. Explicit crack-tip fields of an extending interface crack in an anisotropic bimaterial. Int J Solids Structures 1991;27:455–66.
[14] Qu J, Li Q. Interfacial dislocation and its application to interface crack in anisotropic bimaterials. J Elasticity 1991;26:167–95.
[15] Ni L, Nemat-Nasser S. Interface cracks in anisotropic dissimilar materials: an analytic solution. J Mech Phys Solids 1991;39: 113–44.
[16] Gao H, Abbudi M, Barnett DM. Interfacial crack-tip field in anisotropic elastic solids. J Mech Phys Solids 1992;40:393–416.
[17] Yuuki R, Cho SB. Efficient boundary element analysis of stress intensity factors for interface cracks in dissimilar materials. Engng Fracture Mech 1989;34:179–88.
[18] Lee KY, Choi HJ. Boundary element analysis of stress intensity factors for bimaterial interface cracks. Engng Fracture Mech 1988;29:461–72.
[19] Tan CL, Gao YL, Afagh FF. Boundary element analysis of interface cracks between dissimilar anisotropic materials. Int J Solids Structures 1992;29:3201–20.
[20] Ang HE, Torrance JE, Tan CL. Boundary element analysis of orthotropic delamination specimens with interface cracks. Engng Fracture Mech 1996;54:601–15.
[21] Hong HK, Chen JT. Derivations of integral equations of elasticity. J Engng Mech 1988;114:1028–44.
[22] Portela A, Aliabadi MH, Rooke DP. The dual boundary element method: effective implementation for crack problems. Int J Numer Meth Engng 1992;33:1269–87.
[23] Chen JT, Hong HK. Review of dual boundary element methods with emphasis on hypersingular integrals and divergent series. Appl Mech Rev 1999;52:17–33.
[24] Pan E, Amadei B. Fracture mechanics analysis of cracked 2-D anisotropic media with a new formulation of the boundary element method. Int J Fracture 1996;77:161–74.
[25] Pan E. A general boundary element analysis of 2-D linear elastic fracture mechanics. Int J Fracture 1997;88:41–59.
[26] Lekhnitskii SG. Theory of elasticity of an anisotropic body, San Francisco: Holden-Day, 1963.
[27] Eshelby JD, Read WT, Shockley W. Anisotropic elasticity with applications to dislocations theory. Acta Metal 1953;1:251–9.
[28] Stroh AN. Dislocations and cracks in anisotropic elasticity. Philos Mag 1958;7:625–46.
[29] Ting TCT. Anisotropic elasticity: theory and applications, New York: Oxford University Press, 1996.
[30] Pan E, Chen CS, Amadei B. A BEM formulation for anisotropic half-plane problems. Engng Anal Boundary Elements 1997;20:185–95.
[31] Pan E. A BEM analysis of fracture mechanics in 2-D anisotropic piezoelectric solids. Engng Analy Boundary Elements 1999;23:67–76.
[32] Sollero P, Aliabadi MH, Rooke DP. Anisotropic analysis of cracks emanating from circular holes in composite laminates using the boundary element method. Engng Fracture Mec 1994;49:213–24.
[33] Cruse TA. Boundary element analysis in computational fracture mechanics, Dordrecht: Kluwer Academic, 1988.
[34] Aliabadi MH. Boundary element formulations in fracture mechanics. Appl Mech Rev 1997;50:83–96.
[35] Crouch SL, Starfield AM. Boundary element methods in solid mechanics, London: George Allen and Unwin, 1983.
[36] Tsamasphyros G, Dimou G. Gauss quadrature rules for finite part integrals. Int J Numer Methods Engng 1990;30:13–26.
[37] Isida M, Noguchi H. Plane elastostatic problems of bonded dissimilar materials with an interface crack and arbitrarily located cracks. Trans Jap Soc Mech Engng 1983;49:137–46 in Japanese.
[38] Dwyer JF, Pan E. Edge function analysis of stress intensity factors in cracked anisotropic plates. Int J Fracture 1995;72:327–42.